



Original article

Thermocells of carbon material electrodes and its performance characteristics

Swathi Manda^a, Annu Saini^a, Salman Khaleeq^a, Ritesh Patel^b, Belal Usmani^b, Seshadri Harinipriya^{c,*}, Barun Pratiher^b, Bimal Roy^b

^a Mechanical Engineering, Indian Institute of Technology Rajasthan, Jodhpur, India

^b Center of excellence in energy, Indian Institute of Technology Rajasthan, Jodhpur, India

^c Center of excellence in systems science, Indian Institute of Technology Rajasthan, Jodhpur, India

ARTICLE INFO

Article history:

Received 11 December 2012

Accepted 31 January 2013

Available online 18 June 2013

Keywords:

Thermocells

Activated charcoal

MWCNTs

Low grade waste heat

Flat cells

ABSTRACT

Thermocells in box and flat cell configurations were demonstrated via simplified design and cost effective materials like activated charcoal and potassium ferri/ferrocyanide solution and MWCNTs respectively. Employing saturated concentrations of potassium ferri/ferrocyanide in aqueous solution as electrolyte in combination with the electrodes resulted in a highly feasible redox-mediated electron transfer. Effects of concentration of potassium ferri/ferrocyanide (0.1 mM, 1 M and 4 M in aqueous medium) on the performance of the devices were analyzed. The electrolyte trapped in agar-agar gel functions as a solid like medium. In the case of box configuration the maximum power density attained being 22.463 W/m² yielding 20–30% of Carnot efficiency and 0.563 W/m² for MWCNT based flat cells reaching 0.5–18% higher than the Carnot efficiency. The efficiency of the thermocells at different ΔT from 30 °C to 130 °C was reported. The power density increased by 14.92 times for activated charcoal thermocell operating in 1 M K₃[Fe(CN)₆]/K₄[Fe(CN)₆] at $\Delta T = 60$ °C in comparison with MWCNT based thermocells at the same ΔT . Other low cost electrode materials like activated charcoal, acetylene black were employed to study the performance of thermocells. Cells were connected in series and parallel to study the feasibility of performance improvement at different ΔT .

© 2013 Brazilian Metallurgical, Materials and Mining Association. Published by Elsevier Editora Ltda. Este é um artigo Open Access sob a licença de [CC BY-NC-ND](https://creativecommons.org/licenses/by-nc-nd/4.0/)

1. Introduction

Thermocells were the most attractive way for conversion of thermal energy to electrical energy and energy management. The vital merits of these systems were (i) absence of moving mechanical parts, (ii) complete and closed usage of electrolyte,

(iii) device lifetime and longevity, (iv) simplicity in fabrication, etc. The major sustainable energy source for thermocells being low grade sensible heat at ΔT below 130 °C available from industrial waste effluent streams, geothermal activity, solar heating, solar thermal power plants, data storage systems, etc. Thermoelectric energy conversion was not feasible even though the solid-state thermoelectrics and Stirling engines

* Corresponding author.

E-mail: shpriya@iitj.ac.in (S. Harinipriya).

Nomenclature

Parameters symbols

η	efficiency of the thermocells
r_{ext}	external resistance
I	current
I_{sc}, I_0	short circuit current
V	electrode potential, voltage
V_{oc}, V_0	open circuit voltage
T	temperature
C	concentration of the electrolyte
K	thermal conductivity
S	Seebeck coefficient
N	number of electrons
F	Faraday's constant
$\Delta S_{\text{B,A}}$	reaction entropy for the redox couple
η_r	relative power conversion efficiency
A	cross-sectional area of the cell
D	the electrode separation distance
ΔT	the temperature gradient between the two electrodes
P_{max}	maximum power output
J_{sc}	current density
T_{h}	temperature of hot electrode
I_{max}	maximum current
$P_{\text{max}}/\Delta T^2$	normalized area power density
$J_{\text{sc}}/\Delta T$	normalized area current density
MWCNTs	Multiwalled Carbon Nanotubes

were investigated in the literature, for efficient and effective harvest of low-grade heat to electrical energy [1], mainly due to the limitations on physical, material properties and high cost [2]. Furthermore, Stirling engine technology possesses demerits such as high initial cost and long-term reliability problems [3]. Thus thermocells utilizing the Seebeck effect of the electrolytes to produce electrical power becomes an attractive alternative for harnessing low-grade heat due to its simple design, direct thermal to electric energy conversion, continuous operation, low maintenance and zero carbon emission [4–6].

Investigation of thermocells to generate electricity through direct conversion of thermal energy was not an unheard phenomenon. Redox-type thermocells with aqueous potassium ferri/ferrocyanide solution had been studied in the literature for several decades [4–13]. The solution fills the space between two inert electrodes which were maintained at different ΔT (Fig. 1). Thermocells are electrochemical cells where the voltage and current varies with the external resistance as $r_{\text{ext}} \rightarrow 0$, $I \rightarrow I_0$ (short circuit current) and as $r_{\text{ext}} \rightarrow \infty$, $V \rightarrow V_0$ (open circuit voltage). The efficiency of the thermocells, η based on Seebeck coefficient depends on temperature T , concentration of the electrolyte c , thermal conductivity k , as

$$\eta = \left(\frac{d\phi^{(s)}}{dT} \right)^2 \left(\frac{Tc^0\lambda^0}{4} \right) \left(\frac{1}{kcp} \right)$$

The working principle of the thermocells has been depicted in Fig. 1. Under steady state conditions, Burrows [14] measured a power density (W) of about 0.9 W/m^2 at a $\Delta T = 50 \text{ K}$.

Quickenden and Vernon [15] measured $w = 0.3 \text{ W/m}^2$ at $\Delta T = 20 \text{ K}$ during the initial stage immediately after loading the cell. Thin layer redox-type cells [16,17] had been under research and development for several years. A value of $w = 2.6 \text{ W/m}^2$ at $\Delta T = 73 \text{ K}$ [16] and $w = 3.2 \text{ W/m}^2$ at $\Delta T = 50 \text{ K}$ [17] were reported as steady-state power densities. In all the previously reported literature the temperature gradients were less than 100 K . The reason could be usage of aqueous electrolyte solutions in atmospheric conditions or cells with no antipressure mechanism. The current work investigates the performance of the cells at temperatures above $303\text{--}403 \text{ K}$. The electrochemical Seebeck effect [18,19] for any redox reaction $B \leftrightarrow ne^- + A$ and the Seebeck coefficient, S , in general was expressed as

$$S = \frac{\partial V}{\partial T} = \frac{\Delta S_{\text{B,A}}}{nF}$$

where V is the electrode potential, T is the temperature, n is the number of electrons involved in the reaction, F implies Faraday's constant, and $\Delta S_{\text{B,A}}$ indicates the reaction entropy for the redox couple [20,15]. Aqueous potassium ferri/ferrocyanide solution had been used as the redox system due to its ability to reversibly exchange one electron per iron atom and produce a large reaction entropy, yielding Seebeck coefficient ($>1 \text{ mV/K}$) and high exchange current [14,16,17,15,21,22]. Heat induced voltage generation in electrochemical cell containing ZnO nanoparticles possessing 498 mV with storage capacity of 60 h and exhibiting 1.06% efficiency of Carnot was already reported in literature [23] at an operating $\Delta T = 30\text{--}50^\circ \text{C}$. Apart from this thermodynamics aspects of thermal, chemical and electrochemical systems were extensively analyzed by several researchers in the literature [24].

The power conversion efficiency of a thermocell as modified by Hu et al. [25], expressed as

$$\eta = \frac{1/4 V_{\text{oc}} I_{\text{sc}}}{Ak(\Delta T/d)}$$

and the relative power conversion efficiency implied as $\eta_r = \eta/(\Delta T/T_{\text{h}})$, where V_{oc} is the open circuit voltage, I_{sc} represents the short circuit current, A indicates the cross-sectional area of the cell, d depicts the electrode separation distance, ΔT is the temperature gradient between the two electrodes, k illustrates the thermal conductivity of the electrolyte (or the effective thermal conductivity of the electrolyte and separator), and T_{h} describes the temperature at the hot side. P_{max} , being $1/4 V_{\text{oc}} I_{\text{sc}}$ and $Ak(\Delta T/d)$ indicate the input thermal energy needed to maintain ΔT . $\Delta T/T_{\text{h}}$ corresponds to the Carnot efficiency.

In the present work we attempt to optimize the efficiency and the cost of construction of the thermocells employing simple design of the cell, electrodes, electrolyte and characterization techniques. This study aimed at fabricating a low cost device that can be practically integrated with industrial pipes, rooftops, solar power plants, etc. for extraction of power from sensible waste heat.

2. Experimental

Aqueous solution of $\text{K}_3\text{Fe}(\text{CN})_6/\text{K}_4\text{Fe}(\text{CN})_6$ trapped in agar-agar gel was employed as electrolyte in the thermocells. The

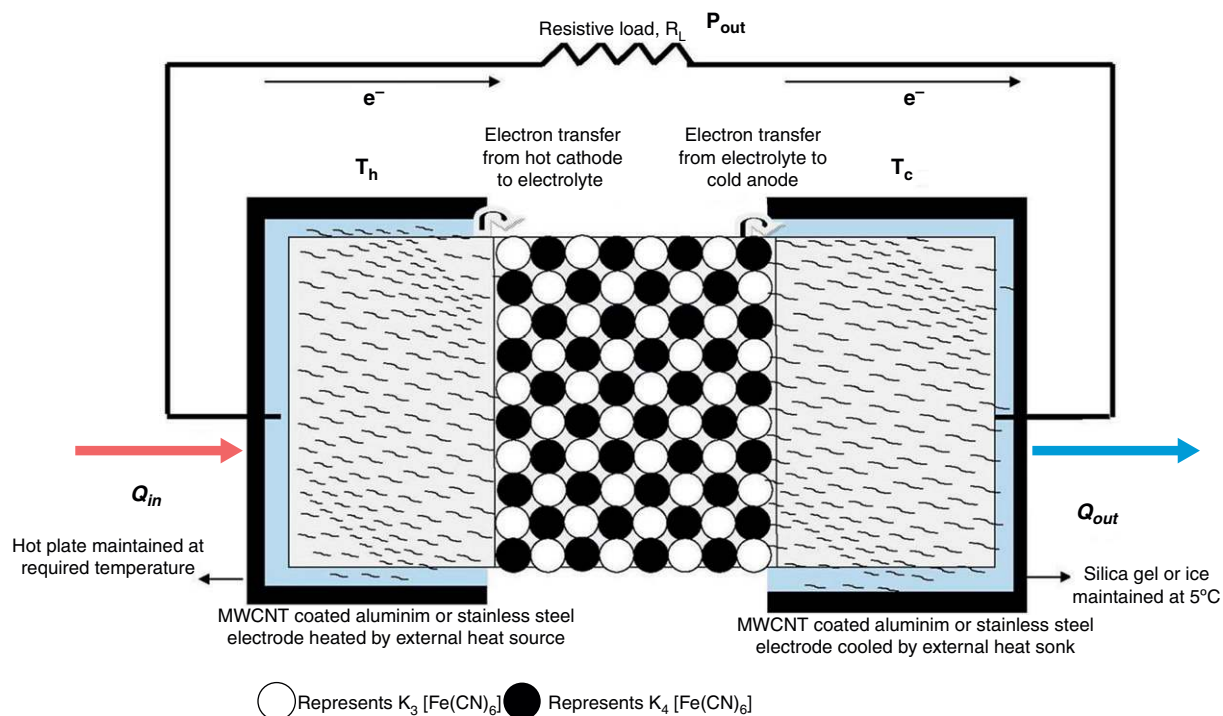


Fig. 1 – Schematic representation of the cross section and working principle of a thermocell.

electrolyte had been studied at different concentrations such as 0.1 mM, 1 M and 4 M. The performance of activated charcoal, acetylene black, acetylene black + copper composite, activated charcoal copper composite (Sigma-Aldrich Co., USA), electrodes were directly compared using a box configuration whereas MWCNTs were used to fabricate flat electrochemical cell. The hot side electrode temperature was maintained at 35–135 °C while the cold side electrode temperature at ~5 °C, the two electrodes were 0.5 cm apart and the electrode dimension being 1.5 cm × 1.5 cm for box configuration and 22 cm × 24 cm for flat cell. The contacts were then covered by insulating M-seal (a chemical mixture of polyurethane resin base, diisodecyl phthalate, xylene, calcium oxide, ethylbenzene and diphenyl methane 4,4' diisocyanate which acts as a sealant) in order to prevent possible artifacts due to interaction between the copper wire and the electrolyte.

3. Construction of thermocell

3.1. Box configuration

Electrode materials (activated charcoal/acetylene black/80% acetylene black + 20% copper powder composite) were pressed and molded as a pellet of radius 1.5 cm and thickness 1.5 cm and effective area of the electrode being 0.007065 m². The pellet was packed in a steel box of similar radius and height. Agar-agar powder (5 g) and appropriate weight of potassium ferri/ferrocyanide were mixed in 50 mL deionized water (Branstead Millipore, USA) depending upon the concentration under consideration (0.1 mM, 1 M and 4 M). The mixed solution was heated at 130 °C on a hot plate with constant stirring till the solution become a gel. The gel was applied

over the activated charcoal electrode and allowed to cool for a day. This packing was then covered by appropriate electrode material pellet and covered by the lid of the box. The copper wires were inserted through the side of the boxes (one at top and other at bottom) and the opening was sealed further by M-seal. K-type thermocouple wires were inserted inside the upper and lower electrode and sealed by M-seal. Thermocouple wires were connected to digital data acquisition system to measure the temperature of hot cathode and cold anode continuously during the experiments. By this setup direct measurement of the temperature of the electrodes was obtained instead of measuring the temperature of heat source and sink. The anode side was sealed with another steel cup to store ice and act as a heat sink. The heat sink was maintained at a temperature of 0–5 °C consistently. Thermocells were heated on the cathodic side using a digital hot plate. I–V discharge characterizations of the prepared thermocells were performed employing iviumstat spectroelectrochemical workstation employing galvanostatic linear sweep voltammetry technique (Fig. 2). The image of typical set up of thermocell has been depicted in Fig. 3.

3.1.1. Flat cell configuration

Slurry of MWCNT in isoamyl acetate was prepared and spread to a thickness of 0.5 cm on an aluminum sheet of 22 cm × 24 cm area and the effective area of the electrode being 0.0528 m². Isoamyl acetate was evaporated from the slurry by allowing the electrode to dry at room temperature. Agar-agar powder (5 g) and appropriate weight of potassium ferricyanide depending upon the concentration under consideration (1 M) were mixed in 50 mL deionized water (Branstead Millipore, USA). The mixed solution was heated at 130 °C on a hot plate

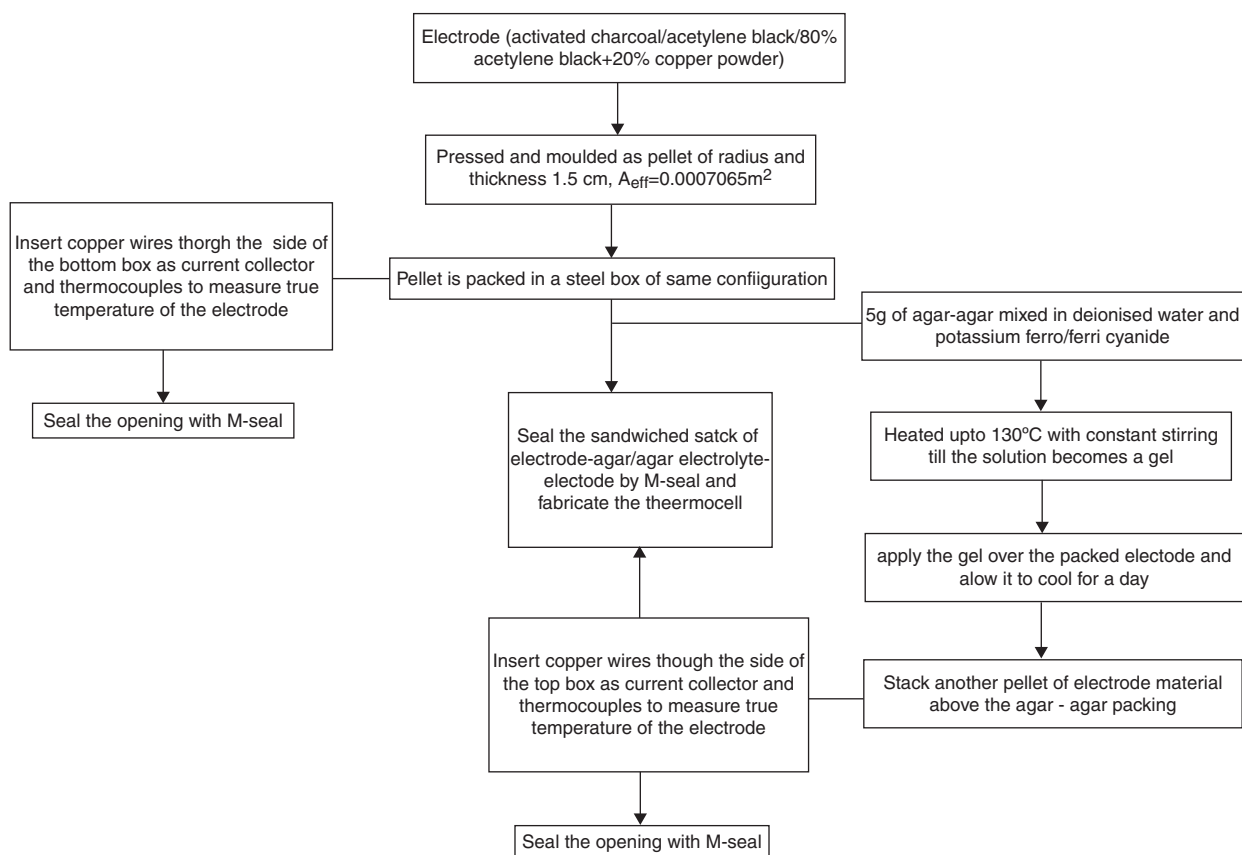


Fig. 2 – Process sheet for construction of thermocell in box configuration.

with constant stirring to form a gel. The gel was applied over the MWCNT electrode and allowed to cool for a day. This packing was then covered by identical MWCNT slurry coated polyethylene sheet on the top. The copper wires were inserted through the side of the cell and sealed by M-seal. K-type thermocouple wires were inserted inside the upper and lower electrode and sealed (Fig. 4). Temperature of the cold side (polyethylene side) always maintained at 5 °C by placing frozen silica gel packs (at 0 °C) over the cell. Image of the flat cell being as depicted below (Fig. 5).

3.1.2. *I-V discharge characterization of thermocells*

The thermocells were heated up to desired temperature and the ΔT maintained till the experiments were completed. At the scan rate of 10 mA/s for box configuration and 20 mA/S for flat cells, the open circuit potential, short circuit current and *I-V* curves were measured employing Galvanostatic Linear sweep voltammetry. The current was kept constant at 10 mA or 20 mA as the case may be and the equilibration time being 30 s to measure the open circuit potential. The cell was discharged before proceeding to another temperature gradient.

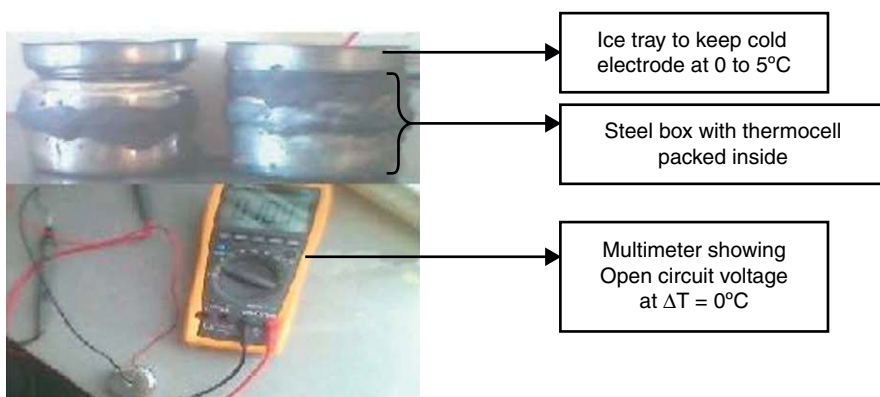


Fig. 3 – The image of typical set up of thermocell.

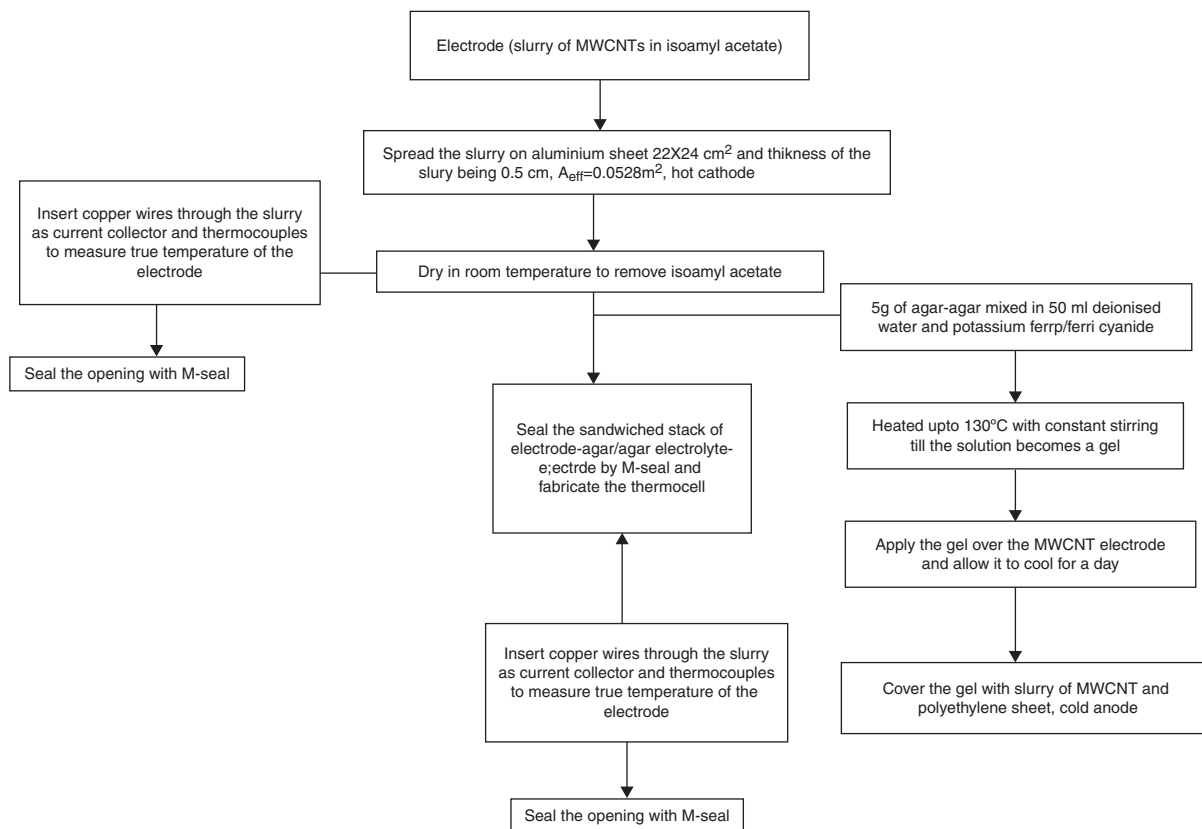


Fig. 4 – Image of the flat cell.

4. Results and discussion

The foregoing analysis indicated that sensible heat can be harnessed and converted to useful power via thermocells employing cost effective materials like activated charcoal, acetylene black copper composite, potassium ferri/ferrocyanide, steel boxes, M-seal and copper wires. Seebeck coefficient of 7.35 mV/K was measured for the activated charcoal electrode, 17.9 mV/K for 80% acetylene black + 20% Cu composite electrode and 20.9 mV/K for MWCNT electrode in 1 M potassium ferricyanide at temperature gradient of 60 °C proving the dependence of Seebeck coefficient on the thermodynamics of the redox couple as well as the thermal conductivity of the electrode material.

4.1. Characterization of 0.1 mM potassium ferri/ferrocyanide and activated charcoal based thermocell

The I-V curve implied the current in mA and negative magnitude due to the discharging of the device. The maximum open circuit potential (V_{oc}) achieved by the device functioning in 0.1 mM electrolyte being 0.6639 V and depending upon the operating ΔT the value of V_{oc} varied from 0.0778 V to 0.6639 V. Fig. 6 depicts that as the ΔT between hot and cold electrodes increases from 30 °C to 120 °C, the performance of the device fluctuated drastically.

Non-linear trend in the performance of the device with the ΔT was observed. At $\Delta T=30-70$ °C, the device showed good performance whereas the performance degradation started from 80 °C to 120 °C. The maximum current up to 10 mA at

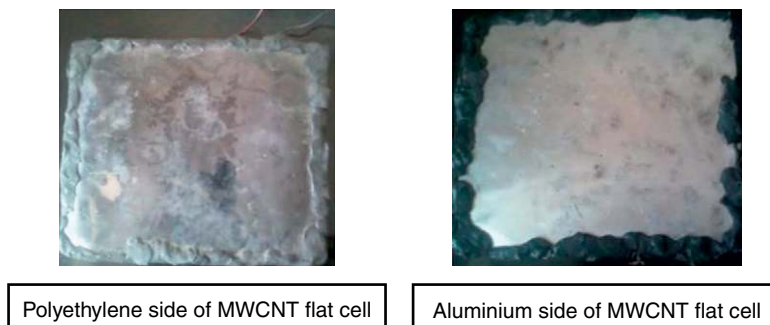


Fig. 5 – Process sheet for construction of thermocell in flat cell configuration.

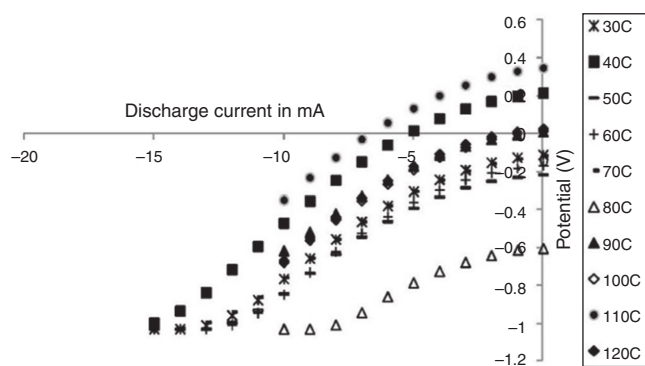


Fig. 6 – I-V discharge characteristics of 0.1 mM electrolyte filled activated charcoal based thermocells.

$\Delta T=80\text{--}120^\circ\text{C}$ and up to 15 mA at $\Delta T=30\text{--}70^\circ\text{C}$ were noticed. The rationale behind this observation may be due to the vaporization of water from the gel at infinite dilution (0.1 mM) and plausible deterioration of the electrolyte beyond 70°C .

At $\Delta T=40^\circ\text{C}$, $P_{\text{max}}=15.92\text{ mW}$ was observed, and the power density approximate to 22.534 W/m^2 . The power density observed being greater than that of ZnO, platinum and MWCNT electrode based thermocells reported in the literature [23,25]. The open circuit potential measured was 0.6639 V with higher I_{sc} and J_{sc} of 4.169 mA and 5.9 A/m^2 , respectively (Table 1). The power conversion efficiency of the device had been calculated employing the equation of Hu et al. [25], where $A=0.0007065\text{ m}^2$, $d=0.005\text{ m}$, k (thermal conductivity of activated charcoal) = 0.51 W/m.K . The maximum power conversion efficiency was observed as 0.024. This value corresponds to ten times lower than the data reported for MWCNT and Pt thermocells [25].

4.2. Characterization of 1 M potassium ferri/ferrocyanide and activated charcoal based thermocell

The effect of concentration of the electrolyte on the performance of the thermocell had been studied by increasing the electrolyte concentration to 10^4 times in the device. The open circuit potential of the device improved drastically with increase in the concentration of the electrolyte. The agar-agar gel was highly saturated with the electrolyte rather than water and resulted in a solid state device. The trend in the parameters such as open circuit potential, short circuit current, current and power density, efficiency and relative efficiency were low at lower temperature gradients from $\Delta T=30\text{--}70^\circ\text{C}$ whereas high at $\Delta T=80\text{--}110^\circ\text{C}$ and again at $\Delta T=120^\circ\text{C}$ the trend falls. Fig. 2 depicts the I-V discharge characteristics of thermocells operating in 1 M electrolyte concentration at different ΔT ranging from 30°C to 120°C . Fig. 7 infers that at higher concentration the trend in I-V characteristics appeared to be inverse to that of 0.1 mM operated thermocells. This could be attributed to the better heat conduction in solid phase device.

Thermocells show better performance at $\Delta T=100^\circ\text{C}$ and 110°C , and beyond 110°C its performance degraded. The P_{max} of the device was measured to be 15.145 mW at $\Delta T=110^\circ\text{C}$ and the power density being 21.44 W/m^2 . The open circuit

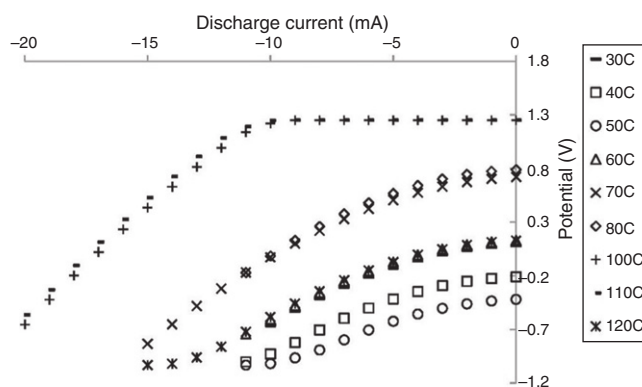


Fig. 7 – I-V discharge characteristics of activated charcoal based thermocell operating in 1 M ferro/ferri electrolyte.

potential measured to be 1.35 V with higher I_{sc} and J_{sc} values of 14.331 mA and 20.2845 A/m^2 , respectively in comparison to the 0.1 mM operated thermocells. The current density J_{sc} possessed the same order as reported but approximately three times lesser than the value obtained for MWCNT and two times lesser than that of Pt based thermocells. The maximum power conversion efficiency of 0.0671 observed at $\Delta T=100^\circ\text{C}$, being three times lower than the value reported for MWCNT and Pt thermocells whereas improved by three times in comparison with 0.1 mM operated device. Analogously, three times improvement in the power conversion efficiency, two times in open circuit potential were noticed with respect to the 0.1 mM operated devices (Table 2). It had been noticed 10^3 order of magnitude increment in the thermal stability of the device. Further improvement on the current density can be attained by changing the electrode material and by increasing the electrode area.

4.3. Characterization of activated charcoal based thermocell in 4 M potassium ferri/ferrocyanide

Thermocells made of activated charcoal electrodes and 4 M ferri/ferro electrolyte had been investigated to understand the threshold limit of concentration of the electrolyte on the device performance. Fig. 8 depicts the performance

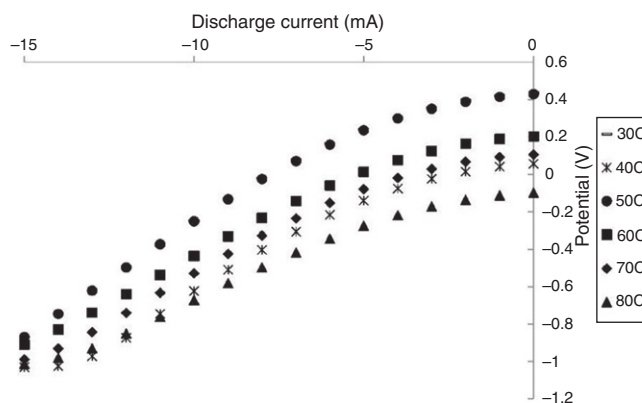


Fig. 8 – I-V discharge characteristics of activated charcoal based thermocell operating in 4 M ferro/ferri electrolyte.

Table 1 – Characterization of 0.1 mM potassium ferri/ferrocyanide and activated charcoal based thermocell.

ΔT (C)	J_{sc} (A/m ²)	I_{sc} (mA)	E_{oc} (V)	P_{max} (mW)	P_{max}/A (W/m ²)	S	Power conversion efficiency	Carnot efficiency	Relative efficiency
30	-1.031	-0.7288	0.0717	14.29	20.22646851	0.00239	0.017948734	0.983766234	1.82E-02
40	-5.9	-4.169	0.6639	15.92	22.53361642	0.016598	0.920320618	0.98427673	9.35E-01
50	0.1809	0.1278	-0.0139	13.95	19.74522293	-0.00028	0.00057239	0.984756098	5.81E-04
60	-0.4911	-0.3469	0.0388	13.78	19.50460014	0.000647	0.004206692	0.985207101	4.27E-03
70	-0.949	-0.6707	0.0653	14.48	20.49539986	0.000933	0.013289122	0.985632184	1.35E-02
80	3.976	2.809	-0.4644	9.611	13.60368011	-0.00581	0.384607873	0.98603352	3.90E-01
90	-2.369	-1.674	0.1208	6.608	9.353149328	0.001342	0.057978195	0.986413043	5.88E-02
100	-2.419	-1.709	0.1345	7.31	10.3467799	0.001345	0.06413638	0.986772487	6.50E-02
110	-2.419	-7.09	0.3345	3.51	4.968152866	0.003041	0.644454868	0.987113402	6.53E-01
120	-2.678	-1.892	0.1485	7.215	10.21231423	0.001238	0.074405315	0.987437186	7.54E-02

Table 2 – Characterization of 1M potassium ferri/ferrocyanide activated charcoal based thermocell.

ΔT (C)	J_{sc} (A/m ²)	I_{sc} (mA)	E_{oc} (V)	P_{max} (mW)	P_{max}/A (W/m ²)	S	Power conversion efficiency	Carnot efficiency	Relative efficiency
30	-0.9146	-0.6469	0.388	6.378	9.027600849	0.012933	0.00290252	0.983766234	0.00295
40	0.65	0.4592	-0.0448	11.45	16.20665251	-0.00112	0.000178422	0.98427673	0.000181
50	3.013	2.129	-0.2606	11	15.56970984	-0.00521	0.00384953	0.984756098	0.003909
60	-4.715	-3.331	0.4407	9.033	12.78556263	0.007345	0.00848778	0.985207101	0.008615
70	-14.15	-10.331	0.307	13.033	18.4472753	0.004386	0.015718474	0.985632184	0.015948
80	-14.15	-10.331	0.787	2	2.830856334	0.009838	0.035257765	0.98603352	0.035757
100	-20.2845	-14.331	1.35	13	18.40056617	0.0135	0.067117834	0.986772487	0.068018
110	-20	-14.13	1.35	15.145	21.43665959	0.012273	0.060160428	0.987113402	0.060946
120	-4.843	-3.421	0.3449	14.9	21.08987969	0.002874	0.003411086	0.987437186	0.003454

Table 3 – Characterization of activated charcoal based thermocell in 4M potassium ferri/ferrocyanide.

ΔT (C)	J_{sc} (A/m ²)	I_{sc} (mA)	E_{oc} (V)	P_{max} (mW)	P_{max}/A (W/m ²)	S	Power conversion efficiency	Carnot efficiency	Relative efficiency
30	-8.9469	-6.321	0.4049	15	21.23142251	0.013497	0.029596475	0.983766234	0.03008
40	-3.733	-2.637	0.2542	14.85	21.01910828	0.006355	0.00581371	0.98427673	0.00591
50	-9.03	-6.38	0.8118	14.06	19.90092003	0.016236	0.035935806	0.984756098	0.03649
60	-6.152	-4.346	0.593	14.5	20.52370842	0.009883	0.014901186	0.985207101	0.01512
70	-5.002	-3.534	0.5258	15.53	21.98159943	0.007511	0.009209091	0.985632184	0.00934
80	-10.64	-7.519	0.835	15.04	21.28803963	0.000798	0.002080264	0.98603352	0.00211

characterization of thermocells at 4M concentration of the electrolyte. From Table 3, the performance of the thermocell appeared uniform and identical for $\Delta T=30-80^{\circ}\text{C}$ thereby demonstrating the thermal stability of the device up to 80°C . $P_{max}=15.53\text{mW}$ was observed at $\Delta T=70^{\circ}\text{C}$ and the power density measured to be 21.98W/m^2 . The open circuit potential of 0.835V measured for the device, with I_{sc} and J_{sc} values as 7.519mA and 10.64A/m^2 , respectively, in comparison with the 0.1mM operated thermocells. In comparison to the current density J_{sc} measured for the MWCNT based device the present thermocell possessed J_{sc} approximately six times lesser value and four times lower value than that of Pt based thermocells [25]. The maximum power conversion efficiency was observed as 0.0359 (Table 3) and being eight times lower than the value reported for MWCNT and Pt thermocells whereas two times lower in comparison with 0.1mM operated device. Although there was tremendous scope for utilizing the device at $\Delta T < 80^{\circ}\text{C}$ no improvement had been noticed in the power conversion efficiency, open circuit potential and the thermal stability of the device with increase in the electrolyte concentration to 4M .

4.4. Dependence of open circuit potential on ΔT and concentration of the electrolyte

Fig. 9 depicts the dependence of open circuit potential of the activated charcoal based thermocell on ΔT and concentration of the electrolyte. The trend in the open circuit potential of thermocells operating at different concentrations of the electrolyte with ΔT exhibit irregularity, even though a window of

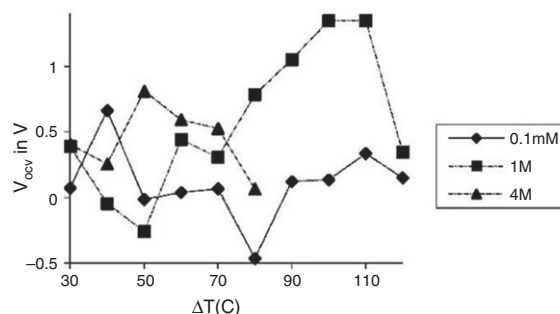


Fig. 9 – ΔT and concentration of the electrolyte dependency of open circuit potential.

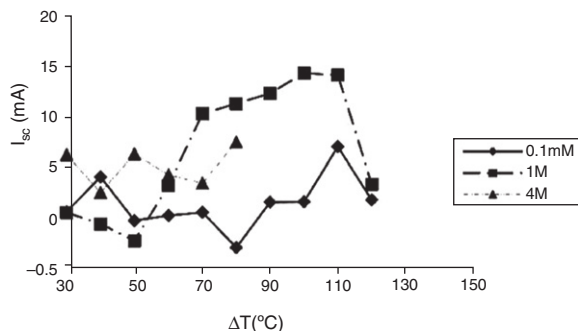


Fig. 10 – ΔT and concentration of the electrolyte dependency of short circuit current.

small ΔT was maintained. For example, thermocell operating at 0.1 mM electrolyte concentration possessed the open circuit potential, V_{oc} of the order of 0.01 V at ΔT 30 °C, 50–100 °C and 120 °C, whereas at 40 °C and 110 °C an increase in V_{oc} being noticed (0.6639 V, 0.3345 V respectively). The rationale behind this anomalous behavior of the device, at $\Delta T=110^\circ\text{C}$, could be attributed to the fact that water in the electrolyte would have got vaporized and hence allowing solid phase electron transfer.

Analogously, in 1 M electrolyte concentration initial decrease in the value of V_{oc} with increase in ΔT occurred from 30 °C to 50 °C. From $\Delta T=60^\circ\text{C}$ to 110 °C V_{oc} increased linearly and decreased drastically at $\Delta T=120^\circ\text{C}$. This trend in V_{oc} with ΔT could be attributed to the solid phase redox reaction at ΔT ranging from 60 °C to 110 °C and degradation of the agar-agar gel and the electrolyte beyond 110 °C.

For thermocells operating at 4 M electrolyte concentration, as the cell opened up beyond 80 °C, a regular trend in V_{oc} was not observed. The data obtained at the rest of ΔT ranging from 30 °C to 80 °C showed entirely reverse trend in comparison to those cells operating in lower concentration of the electrolyte. This may be due to the instability of the concentrated electrolyte toward thermal gradient imposed on the thermocells during their operation.

4.5. Dependence of short circuit current on ΔT and concentration of the electrolyte

Fig. 10 represents the dependence of short circuit current, I_{sc} of the thermocells operating at all electrolyte concentrations and ΔT . Identical trend between I_{sc} and V_{oc} at all

concentrations of the electrolyte as well as ΔT had been observed. This clearly proved that the observed identical effect of the electrolyte concentration on V_{oc} and I_{sc} being analogous to I and V interrelated via Butler–Volmer kinetics for other electrochemical systems.

4.6. Dependence of maximum power output and power density on ΔT and concentration of the electrolyte

The trend in P_{max} and the power density with electrolyte concentration and ΔT are shown in Fig. 11. The maximum power output by thermocells operating at 0.1 mM electrolyte concentration remained constant from 30 °C to 70 °C and falls rapidly with increase in ΔT from 80 °C to 120 °C. This could be attributed to the vaporization of water from the dilute electrolyte leading to performance degradation of the thermocell. Initial P_{max} value at $\Delta T=30-70^\circ\text{C}$ being approximately 13.78–15.92 mW and falls suddenly to 5 mW at 80 °C and fluctuated between 9.611 and 3.51 mW throughout the experiment. Least value of 3.51 mW was noticed at $\Delta T=110^\circ\text{C}$. Analogous trend had been noticed for power density also. The power density remained constant from 30 °C to 70 °C and decrease rapidly with increase in ΔT from 80 °C to 120 °C. Power density value showed less variation initially of around 20 W/m², as the ΔT increases, power density falls to 10 W/m² and then to 3 W/m² indicating the instability of the device at higher ΔT . The reason behind this trend could be due to the change in thermionic processes beyond $\Delta T=80^\circ\text{C}$. In the case of thermocells operating in 1 M electrolyte concentration, although P_{max} and power density are higher than the cell operating at 0.1 mM electrolyte, the trend between P_{max} vs ΔT and power density vs ΔT remain unaltered. For thermocells operating in 4 M electrolyte, the P_{max} and power density measured being 14.06–15.53 mW at $\Delta T=30-80^\circ\text{C}$ and 19.9–21.98 W/m², respectively. This trend indicated that thermocells operating in this concentration range of the electrolyte were more efficient as it attains higher P_{max} and power density at lower temperature gradient. But the safety issues associated with the opening of the seals and the cell leading to cyanide evolution were hazardous and hence cannot be pursued further.

The characterization of activated charcoal electrode based thermocells with optimal electrolyte concentration as 1 M potassium ferricyanide solution trapped in agar-agar gel yielded a maximum power density of 21.437 W/m² at $\Delta T=60^\circ\text{C}$. The value being 14.92 times higher than that of MWCNT based thermocells at the same ΔT . The power from a single thermocell of area 0.000765 m² proved to be insufficient

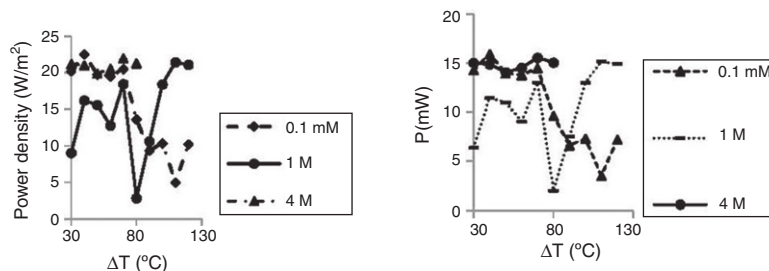


Fig. 11 – ΔT and concentration of the electrolyte dependency on (a) P_{max} (mW) and (b) P_{max}/A (W/m²).

for practical application in small electronic devices like mobile batteries, health care devices, etc. Therefore, different cost effective electrode materials were experimented in a single box-type thermocell. In order to achieve higher power, box-type cells had been connected in series and parallel and characterized at ΔT varying from 30 °C to 120 °C.

5. Construction of thermocell with different electrode materials

Electrolyte used in the current studies being 1M $K_3Fe(CN)_6/K_4Fe(CN)_6$ aqueous solution trapped in agar-agar gel. The construction of box-type cell was done similar to previous study except for the electrodes. The electrode materials employed and their preparation were as follows:

1. Activated charcoal was mixed physically with copper powder in 80:20 wt.% ratio using mortar and pestle.
2. Five cells with activated charcoal as electrode material connected in series with copper wires.
3. A parallel connection of five cells (with activated charcoal and copper as electrode material) was connected with another set of five cells (with activated charcoal and copper as electrode material) in series.
4. Acetylene black was mixed with copper powder in 80:20 wt.% ratio using mortar and pestle.
5. Five cells with acetylene black copper powder composite as electrode material were connected in series.
6. A parallel connection of five cells (with acetylene black mixed with copper powder in 80:20 wt.% ratio as electrode material) in series connected with another set of five cells (with acetylene black mixed with copper powder in 80:20 wt.% ratio as electrode material).

When the mixture appeared fairly uniform, it was pressed and molded as a pellet of radius 1.5 cm and thickness 1.5 cm. The effective area of the electrode was 0.0007065 m² for a single cell and 0.003535 m² for five cells and 0.007065 m² for ten cells. The electrolyte gel was prepared as described in previous study. The hot side temperature was kept constant at 35–125 °C while the cold side temperature was ~5 °C and the two electrodes were 0.5 cm apart. The contacts were then covered by insulating M-seal to prevent possible artifacts due to interaction between the copper wire and the electrolyte.

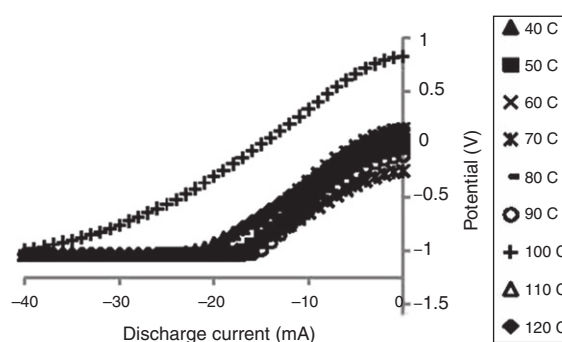


Fig. 12 – I–V discharge characteristics of 80% activated charcoal and 20% copper electrode filled thermocells.

5.1. I–V discharge characterization of thermocells with different electrode materials

The activated charcoal based thermocells were heated up to desired temperature and the ΔT was maintained constant till the experiments were completed. At the scan rate of 10 mA/s, V_{oc} and I–V curves were measured employing Galvanostatic Linear sweep voltammetry. The current varied according to the discharge curve ranging from 15 to 25 mA and the equilibration time was set at 60 s or 90 s to measure the open circuit potential. The cell was then discharged before proceeding to next temperature gradient.

6. Results and discussion

6.1. Characterization of a single 80% activated charcoal and 20% copper powder electrode based thermocell

From the non linear I–V characteristic curves (Fig. 12) and Table 4, it was observed that the maximum V_{oc} obtained being 0.827 V at $\Delta T=100^\circ C$. The trend in the performance observed to be unsteady with respect to the temperature variation and the potential of the device measured to be in the range of 0.01–0.2V at all ΔT . Better results were noticed at $\Delta T=100^\circ C$, but still lower than pure activated charcoal electrode based thermocell which produced, $V_{oc}=1.35 V$. The maximum limiting current the device can withstand approximates to 15 mA at $\Delta T=100^\circ C$. At other temperature

Table 4 – Characterization of a single 80% activated charcoal and 20% copper powder electrode based thermocell.

ΔT (C)	J_{sc} (A/m ²)	I_{sc} (mA)	E_{oc} (V)	P_{max} (mW)	P_{max}/A (W/m ²)	S (mV/K)	Power conversion efficiency	Carnot efficiency	Relative efficiency
40	0	0	-0.027	0	0	-0.00068	0	0.983766234	0
50	-1.41443	-0.001	0.011	2.75E-03	0.00389	0.00022	7.62681E-05	0.98427673	0.000239
60	-6.36492	-0.0045	0.143	0.161	0.227546	0.002383	0.003718071	0.984756098	0.011638
70	0	0	-0.249	0	0	-0.00356	0	0.985207101	0
80	0	0	-0.072	0	0	-0.0009	0	0.985632184	0
90	0	0	-0.1	0	0	-0.00111	0	0.98603352	0
100	-21.2164	-0.015	0.827	3.101	4.386492	0.00827	0.043004826	0.986413043	0.134605
110	-2.82885	-0.002	0.046	0.023	0.032532	0.000418	0.000289945	0.986772487	0.000908

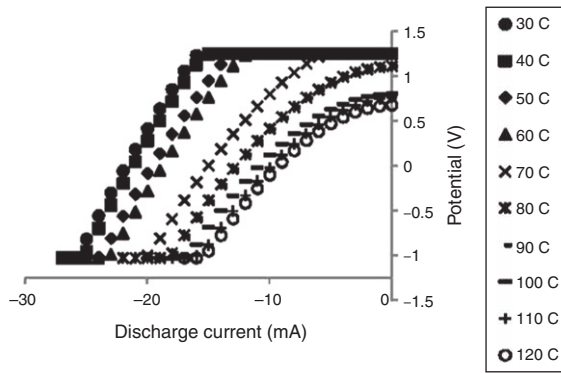


Fig. 13 – I-V discharge characteristics of five activated charcoal electrode filled thermocells in series.

gradients the current decayed to nearly 4 mA. P_{max} produced by the device being 3.101 mW and the maximum power density produced was 4.386 W/m² with a Seebeck coefficient of 0.00827 V/K. The values were nearly five times lower than pure activated charcoal electrode based thermocell which exhibited P_{max} as 15.145 mW and power density as 21.44 W/m². The rationale behind the trend in the performance of the device would be attributed to the electrical and thermal conductivity mismatch of pure activated charcoal and copper coexisting in a non-homogeneous mixture. The difference in phononic vibration frequencies of both the materials may also attribute to the electron transport in the medium resulting in low power as compared to pure activated charcoal electrode based thermocell.

6.2. Characterization of five cells with activated charcoal as electrode material connected in series tested immediately after fabrication

The electrode area being five times that of a single cell i.e. 0.003535 m². The experiment was conducted with an aim to improve the V_{oc} and the maximum power output of the device. From the I-V characteristics (Fig. 13) and Table 5, the maximum V_{oc} was obtained as 1.252 V and the maximum current the device can withstand as 26 mA. The trend showed good performance at ΔT from 30 °C to 70 °C, with degradation after 70–120 °C. This could be attributed to the changes in

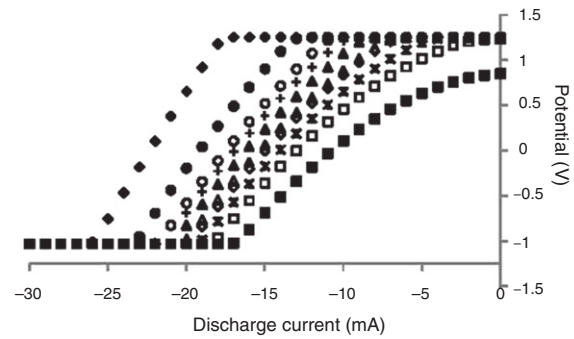


Fig. 14 – I-V discharge characteristics of five activated charcoal electrode filled thermocells in series after 45 days.

electrolyte at high temperatures. The V_{oc} obtained for single cell made of pure activated charcoal at $\Delta T=100-110^{\circ}C$ were captured at ΔT ranging from 30 °C to 70 °C for five cells in series. P_{max} obtained as 6.88 mW and power density of 1.992 W/m² at $\Delta T=30^{\circ}C$ with a Seebeck coefficient of 0.04173 V/K had been measured. These values were three times lesser than the P_{max} of 15.145 mW and ten times less than power density of 21.44 W/m² for a single cell operating at $\Delta T=110^{\circ}C$. The decrement in the power obtained in series could be due to high internal resistance of the copper connecting wires which can be mitigated either by decreasing the length of the wires or by replacing with platinum wires. Feasible and low cost solution would be to increase the electrode area of a single cell instead of connecting many cells in series. Although five cells in series provided lesser power output than single cell, it would be favorable in a sense that if the electrode area had been increased, the device could harness sensible heat even at low ΔT into useful power.

6.3. Characterization of five cells with activated charcoal as electrode material connected in series tested after 45 days

From the characteristic curves (Fig. 14), it was observed that V_{oc} , I_{max} , P_{max} and power density were identical in comparison with single cell tested immediately after fabrication. This uniformity of the values at all ΔT without strong fluctuations implied that the device does not undergo self discharge or

Table 5 – Characterization of 5 cells with activated charcoal as electrode material connected in series tested immediately after fabrication.

ΔT (C)	J_{sc} (A/m ²)	E_{oc} (V)	I_{sc} (mA)	P_{max} (mW)	P_{max}/A (W/m ²)	S	Power conversion efficiency	Carnot efficiency	Relative efficiency
30	-6.22348	1.252	-0.022	0.006886	1.947949	0.041733	0.063658	0.98377	0.064709
40	-5.94059	1.252	-0.021	0.006573	1.859406	0.0313	0.045574	0.98428	0.046302
50	-5.65771	1.252	-0.02	0.00626	1.770863	0.02504	0.034723	0.98476	0.03526
60	-5.37482	1.252	-0.019	0.005947	1.68232	0.020867	0.027489	0.98521	0.027902
70	-4.24328	1.252	-0.015	0.004695	1.328147	0.017886	0.018602	0.98563	0.018873
80	-3.67751	1.11	-0.013	0.003608	1.020509	0.013875	0.012506	0.98603	0.012683
90	-3.67751	1.104	-0.013	0.003588	1.014993	0.012267	0.011057	0.98641	0.011209
100	-3.11174	0.8	-0.011	0.0022	0.622348	0.008	0.006101	0.98677	0.006183
110	-2.82885	0.759	-0.01	0.001898	0.536775	0.0069	0.004784	0.98711	0.004847
120	-2.54597	0.675	-0.009	0.001519	0.429632	0.005625	0.00351	0.98744	0.003555

Table 6 – Characterization of 5 cells with activated charcoal as electrode material connected in series tested after 45 days.

ΔT (C)	J_{sc} (A/m ²)	E_{oc} (V)	I_{sc} (mA)	P_{max} (mW)	P_{max}/A (W/m ²)	S	Power conversion efficiency	Carnot efficiency	Relative efficiency
30	-6.36492	1.252	-22.5	7.043	1.992221	0.041733	0.064460644	0.983766	0.065524
40	-4.24328	1.252	-15	4.695	1.328147	0.0313	0.041600799	0.984277	0.042265
50	-3.11174	0.851	-11	2.34	0.662023	0.01702	0.020094173	0.984756	0.020405
60	-3.67751	1.233	-13	4.007	1.133593	0.02055	0.033374334	0.985207	0.033875
70	-4.52617	1.252	-16	5.008	1.41669	0.017886	0.040493061	0.985632	0.041083
80	-4.24328	1.252	-15	4.695	1.328147	0.01565	0.036886827	0.986034	0.037409
90	-3.9604	1.252	-14	4.382	1.239604	0.013911	0.033479284	0.986413	0.03394
100	-5.37482	1.252	-19	5.947	1.68232	0.01252	0.044218043	0.986772	0.044811
110	-4.9505	1.252	-17.5	0.005478	1.549505	0.011382	0.039663773	0.987113	0.040182
120	-4.80905	1.252	-17	0.005321	1.505233	0.010433	0.037550102	0.987437	0.038028

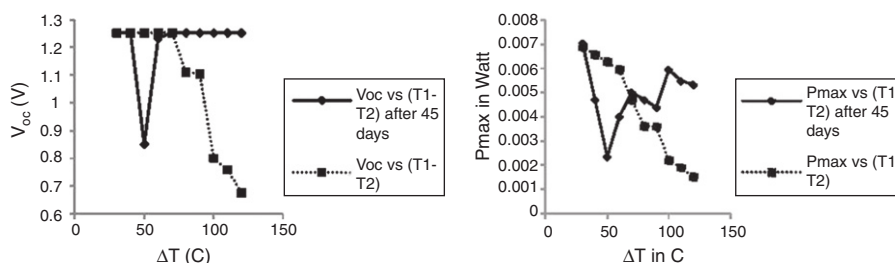


Fig. 15 – (a) V_{oc} and (b) P_{max} vs ΔT of five activated charcoal electrode filled thermocells in series with respect to time.

degradation of chemicals employed over time. Thus thermocell can be a feasible technology for long term usage without performance degradation over time (Table 6).

6.4. Characterization of parallel connection of five cells (with activated charcoal as electrode material) in series connected with another set of five cells (with activated charcoal as electrode material)

The electrode area would be ten times that of a single cell i.e. 0.007065 m². This experiment was carried out with an aim to improve the I_{sc} and P_{max} of the device. From the $I-V$ characteristics (Fig. 15), open circuit potential and I_{max} were observed to be 1.252 V and 22 mA, respectively (Fig. 16). The trend showed steady performance at $\Delta T=70-120^\circ C$. The P_{max} and power density obtained being 6.57 mW and 0.932 W/m², respectively, at $\Delta T=80^\circ C$ with a Seebeck coefficient of 0.01565 V/K. The power obtained being identical to that of a single series of five cells with half the power density. The plausible reason for this behavior might be the internal resistance developed

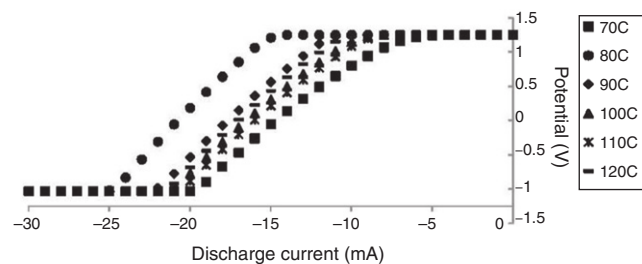


Fig. 16 – $I-V$ discharge characteristics of parallel combination of two series sets of five activated charcoal electrode filled thermocells.

by the copper connecting wires. Hence feasible and low cost solution would be increasing the area of a single cell instead of connecting many cells in series/parallel (Table 7).

6.5. Characterization of a single 80% acetylene black and 20% copper powder electrode based thermocell

From the non linear $I-V$ characteristic curves (Fig. 17), the maximum V_{oc} obtained was 1.252 V which remained constant for the whole range of ΔT studied. The maximum limiting current the device can withstand being nearly constant around 33 mA. The trend of performance observed to be quite steady with the maximum power produced by this device being 7.83 mW and the maximum power density produced was 11.07 W/m² at $\Delta T=80^\circ C$ with a Seebeck coefficient 0.04173 V/K. These values vary very slightly within the range of ΔT employed. The power and power density were nearly

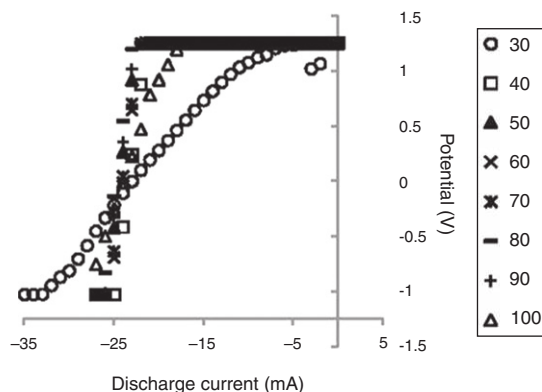


Fig. 17 – $I-V$ discharge characteristics of 80% acetylene black and 20% copper electrode filled thermocells.

Table 7 – Characterization of parallel connection of 5 cells (with activated charcoal as electrode material) in series connected with another set of 5 cells (with activated charcoal as electrode material).

ΔT (C)	J_{sc} (A/m ²)	E_{oc} (V)	I_{sc} (mA)	P_{max} (mW)	P_{max}/A (W/m ²)	S	Power conversion efficiency	Carnot efficiency	Relative efficiency
70	-2.12314	1.252	-15	4.695	0.664544	0.017886	0.01068444	0.98563	0.01084
80	-2.9724	1.252	-21	6.573	0.930361	0.01565	0.01453447	0.98603	0.01474
90	-2.54777	1.252	-18	5.634	0.797452	0.013911	0.01211492	0.98641	0.012282
100	-2.40623	1.252	-17	5.321	0.753149	0.01252	0.01113511	0.98677	0.011284
110	-2.26469	1.252	-16	5.008	0.708846	0.011382	0.01020647	0.98711	0.01034
120	-2.40623	1.252	-17	5.321	0.753149	0.010433	0.01056844	0.98744	0.010703

Table 8 – Characterization of a single 80% acetylene black and 20% Copper powder electrode based thermocell.

ΔT (C)	J_{sc} (A/m ²)	E_{oc} (V)	I_{sc} (mA)	P_{max} (mW)	P_{max}/A (W/m ²)	S	Power conversion efficiency	Carnot efficiency	Relative efficiency
30	-32.5548	1.252	-23	28.796	10.18967	0.041733	0.032947	0.98377	0.03349
40	-32.5548	1.252	-19	28.796	10.18967	0.0313	0.031894	0.98428	0.032403
50	-33.9703	1.252	-17	30.048	10.6327	0.02504	0.03225	0.98476	0.03275
60	-33.9703	1.252	-19	30.048	10.6327	0.020867	0.031282	0.98521	0.031752
70	-33.9703	1.252	-17	30.048	10.6327	0.017886	0.03037	0.98563	0.030813
80	-33.9703	1.252	-17	30.048	10.6327	0.01565	0.029509	0.98603	0.029927
90	-35.3857	1.252	-15	31.3	11.07573	0.013911	0.029892	0.98641	0.030304
100	-33.9703	1.252	-17	30.048	10.6327	0.01252	0.027927	0.98677	0.028302

twice that of activated charcoal copper composite electrode based thermocell (3.101 mW and 4.386 W/m², Table 8). This might be accounted due to higher thermal conductivities of pure acetylene black as compared to pure activated charcoal. Thus acetylene black and copper composite might act as better electrode material than activated charcoal and copper mixture to extract power consistently at both higher and lower ΔT ranges unlike single activated charcoal cell which can extract more power at high ΔT only.

6.6. Characterization of five cells with 80% acetylene black and 20% copper powder electrode based thermocells

From the I-V characteristics (Fig. 18), I_{max} and the maximum V_{oc} were obtained as 23 mA and 1.252 V, respectively. The trend showed good performance at low ΔT (30–40°C), but continuous degradation occurred after $\Delta T=40^\circ\text{C}$ and up to $\Delta T=120^\circ\text{C}$. P_{max} value of 4.7 mW and power density being 0.6645 W/m² at $\Delta T=40^\circ\text{C}$ with a Seebeck coefficient of 0.0313 V/K. The power obtained being lesser than that of

activated charcoal series and power density was three times less than 1.992 W/m² at $\Delta T=30^\circ\text{C}$ (Table 9). This behavior of the device in series may be due to difference in thermal conductivities of pure acetylene black and copper which coexist in a non-homogeneous mixture. The difference in the phononic vibrations frequencies of the materials may lead to reduction in the rate of electron transfer resulting in lower power output compared to pure activated charcoal electrode based thermocell series.

6.7. Dependence of P_{max} on ΔT and electrode assemblies

From Fig. 19, it can be inferred that P_{max} being obtained from a single thermocell of different electrode assembly combinations. The trend showed that there are fluctuations in P_{max} over all ΔT range and higher the ΔT (100°C or 110°C) higher would be the power output of a single cell. On the other hand, a drastic fall in P_{max} being observed in the case of activated charcoal and copper composite with practically negligible power at almost all ΔT except at 100°C. The series and parallel combinations of five and ten activated charcoal

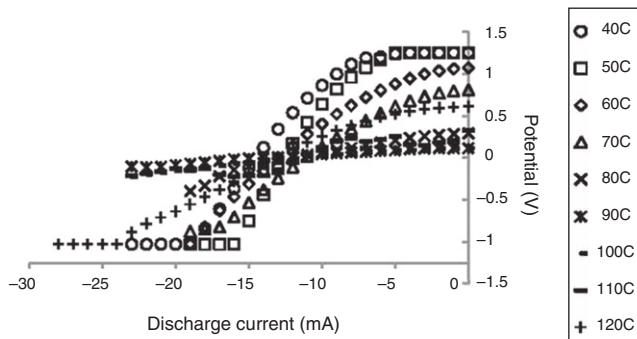


Fig. 18 – I-V discharge characteristics of five 80% activated charcoal and 20% copper electrode thermocells in series.

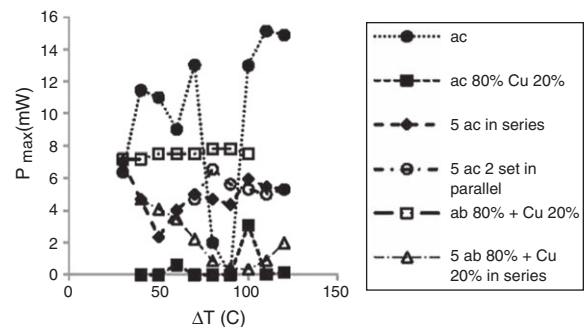


Fig. 19 – P_{max} vs ΔT characteristics of different electrode assemblies.

Table 9 – Characterization of 5 cells with 80% acetylene black and 20% Copper powder electrode based thermocells.

ΔT (C)	J_{sc} (A/m ²)	E_{oc} (V)	I_{sc} (mA)	P_{max} (mW)	P_{max}/A (W/m ²)	S	Power conversion efficiency	Carnot efficiency	Relative efficiency
30	-2.12314	1.252	-0.015	4.7	0.66454	0.0313	0.00416	0.98428	0.004227
40	-1.84006	1.252	-0.013	4.07	0.57594	0.02504	0.003494	0.98476	0.003548
50	-1.84006	1.072	-0.013	3.48	0.49314	0.017867	0.002902	0.98521	0.002945
60	-1.55697	0.809	-0.011	2.22	0.3149	0.011557	0.001799	0.98563	0.001825
70	-1.69851	0.289	-0.012	0.87	0.12272	0.003613	0.000681	0.98603	0.000691
80	-1.9816	0.115	-0.014	0.4	0.05697	0.001278	0.000308	0.98641	0.000312
90	-1.69851	0.117	-0.012	0.35	0.04968	0.00117	0.000261	0.98677	0.000264
100	-1.55697	0.323	-0.011	0.89	0.12573	0.002936	0.000643	0.98711	0.000652

thermocells generated power approximately 33% of that produced from a single activated charcoal thermocell at higher ΔT . The P_{max} from acetylene black and copper powder composite observed to be a constant value at different ΔT ranges, but still lesser than P_{max} from pure activated charcoal cell. Alternatively, combination of acetylene black and copper cells five in series can capture very low ΔT to produce substantial amount of power but the device do not perform well at higher ΔT .

6.8. Dependence of maximum power density on ΔT and electrode assemblies

The trend in Fig. 20 being similar to P_{max} in Fig. 19 except for the difference in scale of the parameters plotted.

6.9. Dependence of efficiency on ΔT and electrode assemblies

According to Fig. 21, at low ΔT , efficiency of activated charcoal cells in series observed to be high and drastically falls with increment in ΔT . On the other hand, activated charcoal electrode based thermocell had higher efficiencies at higher ΔT . The trend in acetylene black thermocells showed that higher efficiencies were obtained at lower ΔT and slowly reduced as ΔT increased. All other assemblies showed identical trend as a single activated charcoal thermocell. It must be noted that though actual efficiencies were lesser than 1%, the efficiency accounts for approximately 20–30% of Carnot efficiency.

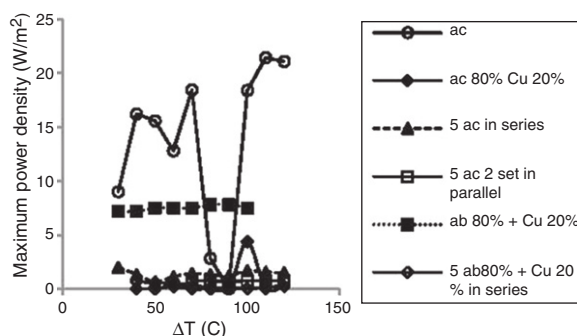


Fig. 20 – Maximum power density vs ΔT characteristics of different electrode assemblies.

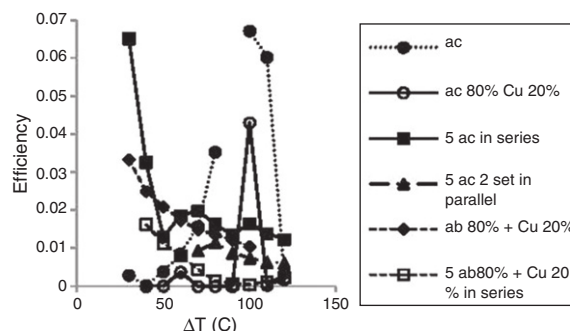


Fig. 21 – Efficiency vs ΔT characteristics of different electrode assemblies.

6.10. Dependence of J_{sc} on ΔT and electrode assemblies

From Fig. 22, it could be seen that high and uniform power density were observed in case of single acetylene black-copper composite electrode based thermocell. The trend can be reasoned by the availability of free electrons in sp^2 hybridized orbitals of acetylene black and d electrons in copper. These electrons contribute to high electron transfer rate and current density. Conversely, combination of such cells in series had very low current density. Activated charcoal single cells showed sudden increase in J_{sc} at ΔT ranging from 100 °C to 110 °C.

From all the above described studies, it could be concluded that the best performance characteristic at high ΔT had been shown by acetylene black single cell while acetylene black and copper composite electrode based single cell generated better and uniform performance characteristic at lower ΔT . The series and parallel connected cells although showed

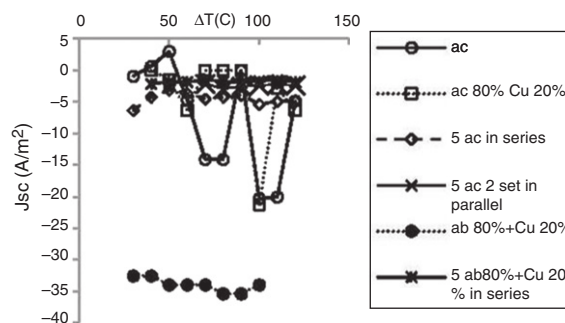


Fig. 22 – J_{sc} vs ΔT characteristics of different electrode assemblies.

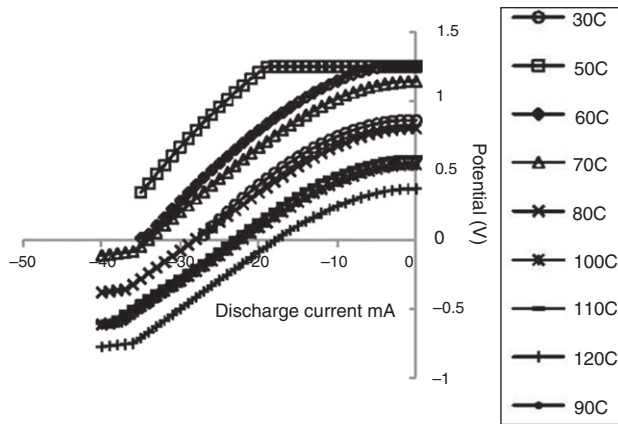


Fig. 23 – V vs I characteristics of flat cell using CNT as electrode material.

consistent results, it was not significant due to high internal resistance developed in the device.

Thus from the experimental results it can be inferred that activated charcoal generated higher power output at high ΔT_s and acetylene black produced high power output at low ΔT_s . When the cells were connected in series and parallel, huge power dissipation happened due to the copper connecting wires. Consequently, it was concluded that instead of connecting cells in parallel or series, utilizing highly conducting materials like multi wall carbon nanotube coatings on a flat flexible plate with large surface area would mitigate both low power output and high internal resistance effects.

7. Characterization of flat cell with CNT as electrode material

A flat and flexible cell was prepared using Aluminum sheet of 0.3 mm thickness, 4 cm \times 4 cm area as hot anode side, plastic transparency sheet of 0.3 mm thickness and 4 cm \times 4 cm area as cold cathode side. A paste made of CNT and acetone was spread evenly using a spatula on each of these sheets up to a thickness of 0.5 cm. $K_3Fe(CN)_6/K_4Fe(CN)_6$ aqueous solution trapped in agar-agar gel was then applied over the dried surface of one of the electrodes and this whole assembly was sealed using M-seal on all four sides.

From Fig. 23 it can be inferred that the I-V characteristics showed a very uniform and well defined trend. V_{oc} was maximum at $\Delta T=40^\circ C$ and $\Delta T=50^\circ C$ with a value of 1.252 V while maximum I_{sc} was at 0.04 A, $P_{max}=0.0109$ W, while maximum power density equals to 6.84 W/m², maximum J_{sc} as 21.875 A/m² and the Seebeck coefficient of 0.02504 V/K at $\Delta T=40-50^\circ C$ (Table 10).

7.1. Characterization of MWCNT based flat cell (1 M potassium ferri/ferrocyanide)

The current dimension investigated being 22 cm \times 24 cm. Fig. 24, implied that the V_{oc} of MWCNT based flat cell being consistently at 1.252 V on all ΔT . The trend in I-V characteristics was uniform without any fluctuation. I_{sc} varies from 20 to 40 mA within the range of ΔT considered.

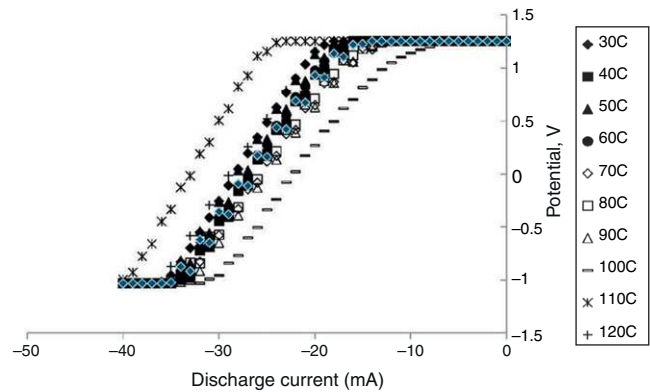


Fig. 24 – I-V characteristics of 22 cm \times 24 cm MWCNT based flat thermocell.

From Fig. 25, irrespective of ΔT , V_{oc} appeared to be a straight line (constant). The maximum voltage fluctuated between 1.252 V and 1 V for ΔT from $30^\circ C$ to $130^\circ C$. The fall of maximum voltage decreased to 1 V at $\Delta T=100^\circ C$ and increased again to 1.252 V at $\Delta T=110-130^\circ C$. The trend in power density and current density is identical with respect to ΔT . Both J_{sc} and power density were in the range of 0.4 A/m² (W/m²) to 0.2 A/m² (W/m²) with a drop noticed at $\Delta T=100^\circ C$ and subsequent increase to initial value. The values I_{sc} and I_{max} overlapped and lie between 20 mA and 40 mA at all ΔT . From Fig. 26a and Table 11, it can be inferred that 20–65% Carnot efficiency being achieved by the device at ΔT ranging from $30^\circ C$ to $100^\circ C$. At $\Delta T=120^\circ C$ and $130^\circ C$, the device power conversion and relative efficiency became equal to that of Carnot efficiency. The device power conversion and relative efficiencies were 2% higher than Carnot efficiency at $\Delta T=120^\circ C$ and 2% lower than Carnot efficiency at $\Delta T=130^\circ C$. At $\Delta T=110^\circ C$, the power conversion efficiency and relative efficiencies of the thermocell were approximately 18% higher than the Carnot efficiency. This high efficiency could be attributed to the plausible change in the thermionic processes at higher temperatures and high thermal conductivity of MWCNTs. The error analysis on power conversion efficiency of MWCNT based flat thermocell by conducting the characterization studies after 120 and 180 days of the fabrication from Fig. 26b. It was seen that the reproducibility of the data lies well within the experimental error limit and the performance of the device remained unaffected after 180 days from the day of its fabrication.

Thus from the above results, it can be concluded that MWCNT based flat cells performs efficiently than any other devices investigated in the current work. Although the maximum power density achieved by the device being ~ 0.6 W/m², the consistent performance of the device at all temperature gradient need to be highlighted.

8. Cost analysis of the device

As the cost of MWCNTs have gone down a lot, in the current market MWCNTs of 10–20 nm size and >95% purity obtained from Chinese academy of Sciences was sufficient to produce

Table 10 – Characterization of flat cell with CNT as electrode material.

ΔT (C)	J_{sc} (A/m ²)	E_{oc} (V)	I_{sc} (mA)	P_{max} (mW)	P_{max}/A (W/m ²)	S	Power conversion efficiency	Carnot efficiency	Relative efficiency
30	-16.875	0.862	-0.027	5.819	3.636563	0.028733	0.118842	0.98428	0.12074
40	-21.875	1.252	-0.035	10.955	6.846875	0.02504	0.134252	0.98476	0.13633
50	-21.875	1.252	-0.035	10.955	6.846875	0.020867	0.111877	0.98521	0.113557
60	-21.25	1.143	-0.034	9.716	6.072188	0.016329	0.085045	0.98563	0.086285
70	-17.5	0.804	-0.028	5.628	3.5175	0.01005	0.043107	0.98603	0.043717
80	-13.75	0.534	-0.022	2.937	1.835625	0.005933	0.019996	0.98641	0.020271
90	-13.75	0.543	-0.022	2.987	1.866563	0.00543	0.0183	0.98677	0.018545
100	-14.375	0.596	-0.023	3.427	2.141875	0.005418	0.01909	0.98711	0.019339

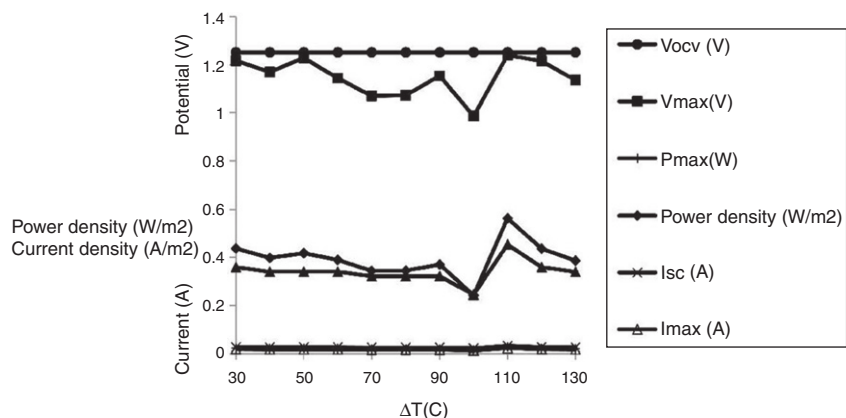


Fig. 25 – Variation of V_{oc} , V_{max} , P_{max} , J_{sc} , power density, I_{sc} and I_{max} of the 22 cm x 24 cm flat thermocell with ΔT .

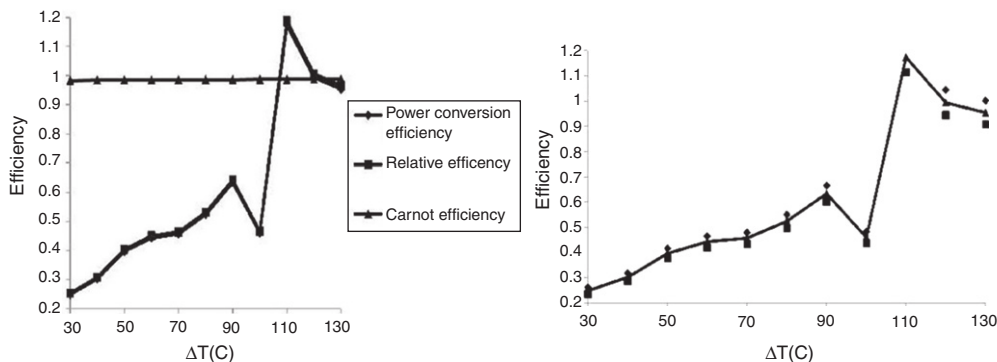


Fig. 26 – Variation of power conversion efficiency and relative efficiency of the device, with Carnot efficiency and ΔT .

Table 11 – Characterization of MWCNT based flat cell (1M potassium ferri/ferrocyanide).

ΔT (C)	J_{sc} (A/m ²)	E_{oc} (V)	I_{sc} (mA)	P_{max} (mW)	P_{max}/A (W/m ²)	S	Power conversion efficiency	Carnot efficiency	Relative efficiency
30	0.3598485	1.252	0.019	0.023123	0.4379356	0.041733	0.248827045	0.983766234	0.252933102
40	0.340909091	1.252	0.018	0.02106	0.398863636	0.0313	0.302169422	0.98427673	0.306996409
50	0.340909091	1.252	0.018	0.022104	0.418636364	0.02504	0.39643595	0.984756098	0.40257273
60	0.340909091	1.252	0.018	0.020592	0.39	0.020867	0.443181818	0.985207101	0.4498362
70	0.321969697	1.252	0.017	0.01819	0.344507576	0.017886	0.456733529	0.985632184	0.463391452
80	0.321969697	1.252	0.017	0.018241	0.345473485	0.01565	0.523444674	0.98603352	0.530858904
90	0.321969697	1.252	0.017	0.019618	0.371553	0.013911	0.633328977	0.986413043	0.642052517
100	0.2462121	1.252	0.013	0.012818	0.2427652	0.01252	0.459782576	0.986772487	0.465945881
110	0.4545455	1.252	0.024	0.029736	0.5631818	0.011382	1.173295417	0.987113402	1.188612589
120	0.3598485	1.252	0.019	0.023085	0.4372159	0.010433	0.9936725	0.987437186	1.006314644
130	0.3409091	1.252	0.018	0.020448	0.3872727	0.009631	0.95351233	0.987745098	0.965342507

0.4 W/m² of power density in a flat cell. Moreover, the other materials employed in the fabrication of the thermocell constituted (i) potassium ferrocyanide and ferricyanide, (ii) agar-agar gel, which cost around Rs. 500/kg. Hence the fabrication cost of a single flat cell of MWCNT electrodes being Rs.10 and the power gained by this expenditure is around 0.4 W/m² approximately 0.22\$ per 0.4 W/m². The cost further came down upon usage of electrode materials like activated charcoal, acetylene black and copper powder. Thus for thermocells made of activated charcoal, acetylene black and copper powder Rs.10 was the expense for a gain of 22 W/m², approximately 0.22\$ per 22 W/m² which in turn being much more cost effective than any other thermocells demonstrated in the literature [25].

9. Perspectives and summary

The performance and efficiency of box configuration thermocells operating in activated charcoal, acetylene black and copper composite electrodes, agar-agar gel trapped potassium ferri/ferricyanide electrolyte had been studied. The Seebeck coefficient of 7.35 mV/K was measured for the activated charcoal electrode at 1M potassium ferricyanide at $\Delta T = 6^\circ\text{C}$ and seven times higher than the value of 1.4 mV/K reported by Hu et al. [25] employing MWCNTs and 0.4M potassium ferricyanide at $\Delta T = 60^\circ\text{C}$, proving the fact that the thermodynamics of the redox couple and electrode material governs the Seebeck coefficient. The J_{sc} and power density (P_{max}) generated by the activated charcoal electrodes in 0.1 mM, 1M and 4M potassium ferricyanide were 3.976 A/m², 20.495 W/m² and 20.2845 A/m², 21.437 W/m² and 9.03 A/m², 21.98 W/m², respectively, whereas that of the other electrode materials were discussed in other sections. The normalized current density at $\Delta T = 60^\circ\text{C}$ for all the three concentrations of electrolyte mentioned above were $J_{sc}/\Delta T$, 0.066 A/m² K, 0.338 A/m² K and 0.151 A/m² K, respectively. The rationale behind this lower value of normalized current density might be due to the lower thermal conductivity of the activated charcoal electrodes. The normalized area power density, $P_{max}/\Delta T^2$ of 5.7×10^{-3} W/m² K², 5.96×10^{-3} W/m² K² and 6.11×10^{-3} W/m² K² for 0.1 mM, 1M and 4M electrolyte respectively were measured. It was reported in the literature that the Pt electrodes generated a J_{sc} of 48.4 A/m² and a P_{max} of 1.02 W/m², corresponding to a $J_{sc}/\Delta T$ of 0.81 A/(m² K) and a $P_{max}/\Delta T^2$ of 2.8×10^{-4} W/(m² K²). The graphite sheet electrodes generated a J_{sc} of 36.6 A/m² and a P_{max} of 0.76 W/m², corresponding to a $J_{sc}/\Delta T$ of 0.61 A/(m² K) and a $P_{max}/\Delta T^2$ of 2.1×10^{-4} W/(m² K²). Hence the current methodology would positively pave way for cost effective tapping of sensible heat and converting it in to useful power.

With different electrode materials, it was concluded that activated charcoal electrode thermocell had produced the highest maximum power of 15.145 mW and power density of 21.44 mW/m² at $\Delta T = 100^\circ\text{C}$. Thus making material best suited for use in industrial applications where waste heat in the range of $\Delta T = 100^\circ\text{C}$ being available. Acetylene black had produced a maximum power of 4.7 mW with maximum power density of 0.6645 mW/m² and current density as 35.38 A/m². By achievement of 18% higher efficiency than Carnot efficiency

at $\Delta T = 110^\circ\text{C}$ for MWCNT based thermocells, real time applications of waste heat harnessing from thermal power plants, solar power plants, processing industries, etc. becomes plausible and best suited to extract the power from low temperature gradients across roofs, panels, bioreactors, etc.

The foregoing analysis aimed at development of thermocells which can harvest the waste heat or low grade sensible heat into useful power. In the current investigation cost of the thermocells had been tremendously brought down by cost effective materials like activated charcoal, boxes made of low quality steel and electrolyte trapped in agar-agar gel. By using optimal concentration of electrolyte as 1M and using appropriate electrode material, the power obtained had been improved by 14.92 times as seen in recent literature. To demonstrate thermocells in harnessing solar heat as well as low grade heat dissipated by storage devices and super computers and converted into power, experiments were performed employing flat cells. The future work in this regard aims at (i) demonstrating the device on flexible substrates in a real time data monitoring environment like exhaust pipes, chimneys, hot water pipes, etc. (ii) Studying the effects of vibrations of the heat transfer pipe on the phononic vibrations in the thermocells, (iii) designing a complete product from scratch, (iv) Integrating power storage devices and charge regulators into thermocells to harness waste thermal energy from solar panels, waste heat from Concentrated solar power plants, thermal heat generated in electronic devices like mobiles, tablets, laptops, etc. Although the current flat and box configuration thermocells produced consistent and constant power output for the maximum of 45 days, operational lifetimes of years to decades would be more desirable. Since the available waste energy being free and unlimited from several sources, relatively high conversion efficiencies of the presently improved thermocells and its cost effectiveness becomes a preferred task in the future.

Conflicts of interest

The authors declare no conflicts of interest.

REFERENCES

- [1] Vining CB. An inconvenient truth about thermoelectrics. *Nat Mater* 2009;8:83-5.
- [2] Mancini T, Heller P, Butler B, Osborn B, Schiel W, Goldberg V, et al. Dish-Stirling systems: an overview of development and status. *J Sol Energy Eng* 2003;125:135-51.
- [3] The Future of Geothermal, Energy. Impact of enhanced geothermal systems (EGS) on the United States in the 21st, century. Massachusetts Institute of Technology; 2006.
- [4] Agar JN. Advances in electrochemistry and electrochemical engineering. New York: Wiley & Sons; 1961.
- [5] Haase R. Thermodynamics of irreversible processes. Boston: Addison-Wesley; 1962.
- [6] Ratkje SK, Ikeshoji T, Syverud K. Heat and internal energy changes at electrodes and junctions in thermocells. *J Electrochem Soc* 1990;137:2088-95.
- [7] Agar JN. Thermogalvanic cells. In: Delahay P, Tobias CW, editors. Advances in electrochemistry and electrochemical engineering. 3rd ed. New York: Wiley & Sons; 1963.

- [8] Christy RW. In: Cadoff IB, Miller E, editors. Thermoelectric materials and devices. New York: Reinhold; 1960 [chapter 12].
- [9] Sundheim BR. In: Cadoff IB, Miller E, editors. Thermoelectric materials and devices. New York: Reinhold; 1960 [chapter 14].
- [10] Peck RL. Ionic semiconductor materials and applications thereof. US Patent 4.797.190; 1989 January 10.
- [11] Peck RL. Thermoelectric energy system. US Patent 4.211.828; 1978 November 9.
- [12] Uhlig HH, Revie RW. Corrosion and corrosion control. New York: Wiley & Sons; 1985.
- [13] Anderson LB, Greenberg SA, Adams GB. Thermally and photochemically regenerative electrochemical systems. In: Crouthamel CE, Recht HL, editors. Regenerative EMF cells. Advances in chemistry, vol. 64. Washington, DC: ACS Publication; 1964.
- [14] Burrows B. Discharge behavior of redox thermogalvanic cells. *J Electrochem Soc* 1976;123:154-9.
- [15] Quickenden TI, Vernon CF. Thermogalvanic conversion of heat to electricity. *Sol Energy* 1986;36:63-72.
- [16] Ikeshoji T. Thermoelectric conversion by thin-layer thermogalvanic cells with soluble redox couples. *Bull Chem Soc Jpn* 1987;60:1505-14.
- [17] Ikeshoji T, Nahui FNB, Kimura S, Yoneya M. Computer analysis on natural convection in thin-layer thermocells with a soluble redox couple: Part 2. E-I relation, electric power, heat flux and electrochemical heat pump. *J Electroanal Chem Interfacial Electrochem* 1991;312:43-52.
- [18] Coggeshall GWZ. *Phys Chem* 1895;24:62-72.
- [19] Richards TWZ. *Phys Chem* 1897;24:39-49.
- [20] Eastman ED. Electromotive force of electrolytic thermocouples and thermocells and the entropy of transfer and absolute entropy of ions. *J Am Chem Soc* 1928;50:292-7.
- [21] Quickenden TI, Mua Y. A review of power generation in aqueous thermogalvanic cells. *J Electrochem Soc* 1995;142:3985-94.
- [22] Mua Y, Quickenden TI. Power conversion efficiency, electrode separation, and overpotential in the ferricyanide/ferrocyanide thermogalvanic cell. *J Electrochem Soc* 1996;143:2558-64.
- [23] Mondal A, Basu R, Das S, Nandy P. Heat induced voltage generation in electrochemical cell containing zinc oxide nanoparticles. *Energy* 2010;35:2160-3.
- [24] Sieniutycz S, Poświata A. Thermodynamic aspects of power production in thermal, chemical and electrochemical systems. *Energy* 2012;45:62-70.
- [25] Hu R, Cola BA, Haram N, Barisci JN, Lee S, Stoughton S, et al. Harvesting waste thermal energy using a carbon-nanotube-based thermo-electrochemical cell. *Nano Lett* 2010;10:838-46.